Density Fluctuations in Liquid Water

Niall J. English[1,*] and John S. Tse[2,†]

[1]*The SEC Strategic Research Cluster and the Centre for Synthesis and Chemical Biology,*
School of Chemical and Bioprocess Engineering, University College Dublin, Belfield, Dublin 4, Ireland
[2]*Department Physics and Engineering Physics, University of Saskatchewan, Saskatoon, Saskatchewan, S7N 5E2, Canada*
(Received 1 September 2010; published 18 January 2011)

The density distributions and fluctuations in grids of varying size in liquid water at ambient pressure, both above the freezing point and in the supercooled state, are analyzed from the trajectories obtained from large-scale molecular dynamics simulations. It is found that the occurrence of low- and high-density regions (LDL and HDL) is transient and their respective residence times are dependent on the size of the simulated system. The spatial extent of density-density correlation is found to be within 7 Å or less. The temporal existence of LDL and HDL arises as a result of natural density fluctuations of an equilibrium system. The density of bulk water at ambient conditions is homogenous.

PACS numbers: 61.25.Em, 61.43.Bn

Bulk water possesses several anomalous behavioral characteristics that cannot be explained easily from the viewpoint of a simple liquid. Recently, the conventional picture on the near-tetrahedral hydrogen-bonded water structure was challenged [1,2]. From the analysis of x-ray absorption [1,2] and emission spectra [3] the surprising conclusion was reached that the water molecule environment in the liquid is highly distorted with two distinct local structures, where a majority of water molecules participated in a strong asymmetrical H-bond and only a minority are tetrahedrally bonded [1]. In other words, the structure of bulk water at ambient conditions is inhomogenous but a mixture of two different entities. Recently, the density difference contrast observed in small-angle x-ray scattering experiments (SAXS) of bulk water measured between 7 to 74 °C were attributed to temperature dependent fluctuations of the two types of local structures [4]. The authors of Ref. [4] further argued that this observation was akin to the postulated liquid-liquid phase transition between high (HDL) and low-density (LDL) water in the supercooled regime [5–9], where the high-density liquid structure is highly distorted and the low-density structure is more tetrahedral. The interpretation provided in Ref. [4] has been highly contested [10,11]. The simultaneous temporal presence of high- and low-density regions in a liquid is not surprising. This could be a manifestation of the natural fluctuation dissipation of a system under thermodynamic equilibrium and the features observed in the recent SAXS study may just be the result of dynamic number fluctuations common to all liquids and not necessary is the consequence of the presence of two distinct components [7,8].

For water to be a mixture of two liquids with distinct structures, it is essential to define the relative concentration and the lifetime of each entity and their temperature dependence. For this purpose, equilibrium molecular dynamics (MD) simulations were performed with 1.07×10^6 water molecules in cubic simulation boxes for 1 ns using the SPC/E model, which has proven to be relatively accurate for estimation of water properties [12]. The particle-mesh Ewald method was used to handle long-range electrostatic interactions [13], to within a relative precision of better than 10^{-5}. Simulations were performed in the canonical ensemble (constant volume-constant temperature, NVT) at 200, 225, and 270 K at densities corresponding to 1 bar pressure, using a light coupling to a Nosé-Hoover thermostat [14], to allow for the possibility of observing phase coexistence [15]. As the freezing point of SPC/E water is ~215 K [16], these temperatures were chosen so as to allow for a study of supercooled liquid water, and the liquid state above freezing (by ~10 and 55 K). The DL-POLY3 code was used [17]. The box length of an initial system was slightly in excess of 316 Å to conform to a density of 1.00 g/cm^3. Constant pressure MD (NPT) was employed to relax the system for 1 ns at each temperature using a light coupling to Melchionna's modified form of the Hoover barostat with isotropic cell fluctuations [18], so as to lead to the appropriate system density corresponding to ambient (1 bar) pressure, prior to production (canonical) simulation. It was found that 1 ns was satisfactory for convergence of the system densities, which were found to be 0.998, 1.011, and 1.010 g/cm^3 at 200, 225, and 270 K, respectively, in good agreement with results of Harrington *et al.* [9] and Bryk and Haymet [19].

The motivations of using a large system are twofold. First, in an MD calculation, the maximum sustainable wavelength of a thermal fluctuation is double that of the shortest dimension of the simulation box. This wave can create compressed and uncompressed regions throughout the liquid leading to density fluctuations, the distribution of which is affected by system size. Second, the large simulation box can be divided into smaller subsystems and the homogeneity of the low- and high-density local structures can be examined.

In analyzing the resultant density fluctuations from MD, a central cubic box of 316 Å side-length (within the slightly larger fixed simulation box length) was divided into $n = 6, 8, 10, 12, 16, 20$, and 32 grids for a total of n^3 elements, and the number of water molecules in each element counted throughout the simulation so as to calculate the densities therein, and corresponding probability distributions were defined across the grid elements. The typical ranges of number of water molecules in each element were 27–39, 125–143, 251–273, 602–640, 1050–1100, 2060–2140, and 4930–5030 from the smallest to largest. Periods of time for which elements had a density $(\rho) < 0.9$ or >1.1 g/cm^3 were designated as instances of low- and high-density, respectively, and a series of persistence times for these particular states were calculated as the elements' densities fluctuated, as well as the overall proportion of simulation time for which each element was in a low- ($\rho < 0.9$ gm/cm^3) or high- ($\rho > 1.1$ gm/cm^3) density state. Probability densities were also defined across all elements for these persistence times and overall proportions of simulation time. In order to corroborate our findings of density fluctuations (*vide infra*), we also simulated a much smaller system of 472 molecules at the three temperatures using identical simulation techniques.

In Fig. 1, the probability distribution of the elements' densities at 270 K are shown. The results at 200 and 225 K have been omitted here due to close similarity: they show similar features with the peaks centered at 0.998 and 1.011 g/cm^3, respectively. It can be seen that the elements' densities are centered closely around the bulk value of 1.010 g/cm^3. The isothermal compressibility in each of the elements containing N molecules, χ, was evaluated from $\langle N \rangle V k_B T \chi = (\langle N^2 \rangle - \langle N \rangle^2)/\langle N \rangle$, and their probability distributions were centered closely on experimental
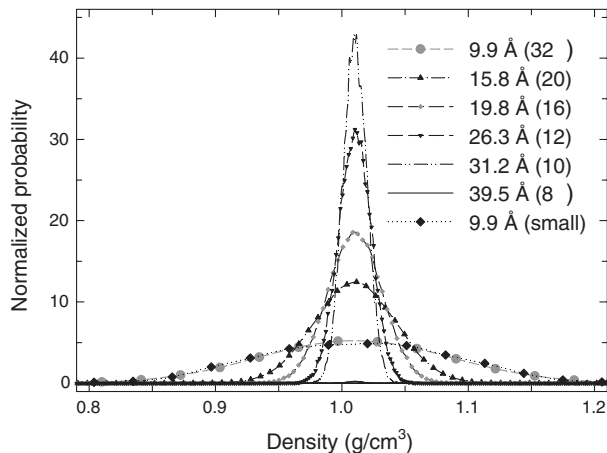
[20] and previous SPC/E-model [21] results; these were 0.45, 0.50, and 0.56×10^{-9} Pa^{-1} at 200, 225, and 270 K, respectively. For the larger cells ($n = 8, 10$ and 12, and corresponding to cell sizes of 39.5, 31.2, and 26.3 Å), the average deviation from the mean distribution is almost constant at ± 0.025 gm/cm^3 and increases slightly to ± 0.04 gm/cm^3 for the 15.8 Å cell. A clear exception to this trend is the 9.9 Å-side length case (for a 32^3 grid) where there is some evidence that there could potentially be regions of low or high density, notwithstanding the possibility of an artifact of fluctuations in counting statistics for such small grid cells which contain only 27–39 molecules. This observation indicates the temporal density variation is only observed in small regions of bulk water and both the LDL and HDL regions should be less than around 1 nm. This was confirmed directly by clustering adjacent high- and low-density elements of half this dimension (i.e., 4.94 Å, with 3–5 molecules therein, and 3 or less as low, and 5 or more as high density), and then defining radii of gyration for the molecules in these clusters of high- and low-density mini-elements for rotation about their overall centers of mass. It was found that the resulting probability distribution of these radii of gyration was centered at 4–5 Å and had no radii beyond 10–12 Å, consistent with no observation of LDL or HDL in 15.8 Å-side elements (cf. Figure 1). However, aside from the temporal existence of clusters of high and low density and the estimation of their size range, whether by grid dimension or radius of gyration, is the matter of the definition of a density correlation length. We estimated this by defining a spatial grid-based density-density correlation function, $\langle \rho(r) \cdot \rho(r') \rangle / \langle \rho(r) \cdot \rho(r) \rangle$ and analyzing its decay with distance between the centers of elements, $r\text{-}r'$. Here, $\rho(r)$ denotes the density of an element in terms of its geometric center as the position, and this correlation function is averaged over all element pairs and over time; it is illustrated in Fig. 2 at 270 K for 9.9 and 4.94 Å-side elements; these elements were chosen as larger ones did not exhibit high or low density. There is clear decay with increasing separation from unity for self-correlation (i.e., elements' own densities at zero separation from themselves) towards essentially zero density correlation beyond around 7 Å. In the case of the 9.9 Å-side elements, the minimum distance between direct neighbors is 9.9 Å, so the 4.94 Å-side mini-elements are necessary to capture the density decay length scale. This lack of density correlation beyond around 7 Å is clearly evident for all temperatures studied. The observation that the density correlation length is around 7 Å or less, coupled with typical radii of gyration of 4–5 Å for HDL-LDL clusters, is consistent with estimates of around 8 and 4 Å for the density correlation length estimated by Bosio *et al.* [22] and Clark *et al.* [23], notwithstanding that the radii of gyration are not a strict measure of density correlation. We conjecture that this length scale arises from the stability of the O-O distance when a hydrogen bond is formed, as this is of the order of the first or second neighbor distance.
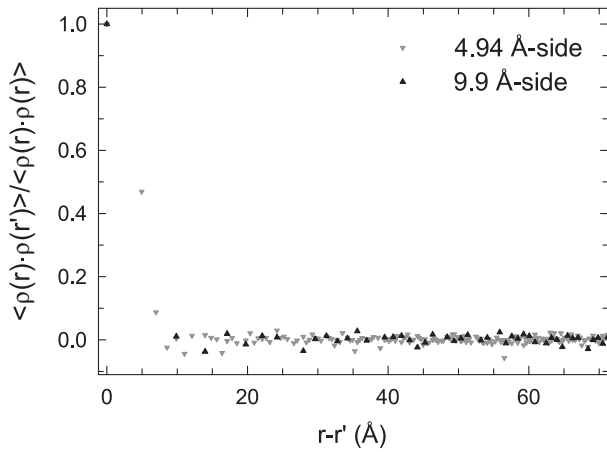

FIG. 1. Normalized probability distributions of density in differently sized grids (with number of n grids per overall 316 Å cubic box length indicated in parenthesis) at 270 K and 1 bar pressure. Results are very similar at 200 and 225 K and for the small system (see text). The data for the 9.9 Å-side elements in the small system are shown, but omitted for clarity in other cases.

FIG. 2.   Normalized grid-based spatial density-density correlation function at 270 K in terms of distance between the centers of the elements in 32^3 and 64^3 grids for the 1.07×10^6-molecule system. The lack of correlation is evident between elements whose centers are more than around 8 Å distant. This varies little with temperature.

FIG. 3.   Normalized probability distributions of persistence times of high-densities in 9.9 Å-side grid elements in the 1.07×10^6-molecule and small systems; these are defined as periods of time of density greater than 1.1 g/cm^3. The distributions for low-density residence times are essentially identical.

To investigate the time scales of the density fluctuations within these LDL and HDL regions, the probability distributions for the persistence times in the elements of high-densities are shown in Fig. 3 for the 9.9 Å-side grid (the only grid for which low- and high-density regions are found); the distributions of low-density residence times are essentially identical, and are omitted for clarity. It can be seen clearly that the low- and high- element densities are transient, lasting only about 4 ps or less at all temperatures studied. This characteristic time is remarkably close to the residence time of a water molecule in the bulk liquid at ambient conditions [24], and simply represents the time required for a water to diffuse out of its local environment. It was found that over 99% of all elements possessed these transient periods of both low- and high-density throughout the simulations at all temperatures, and the probability distributions of the overall proportions of simulation time are shown in Fig. 4. The 9.9 Å-side elements are in the low- and high-density state up to some 15%–20% of the time for each case. It was also observed that the transient instances of low- and high-density states were distributed evenly throughout the simulations. It is significant to note that neither an appreciable increase in persistence times for "low-" and "high-" density regions nor for the overall proportion of simulation time are observed in the supercooled state. This suggests strongly that both liquid and supercooled water is a single-phase liquid at ambient pressure.

An important finding is that the "concentration" of LDL and HDL and their persistence times are dependent on the system size. To illustrate this, results from canonical simulations with a much smaller 472-molecule system, more typical of the size range of neat water systems studied by MD historically, are compared. The smaller system was chosen so that it can also be subdivided into cells of
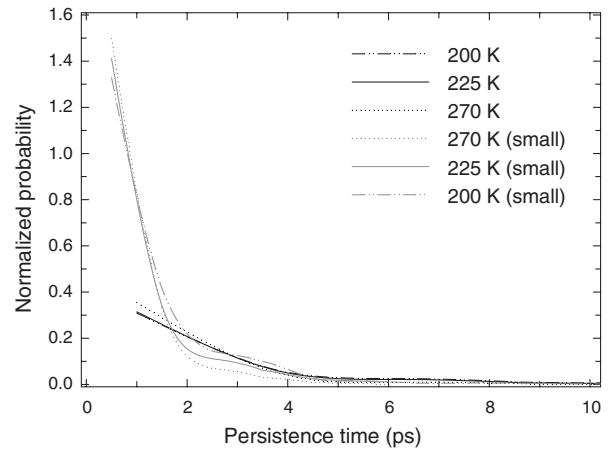
identical dimension to the smaller elements in the large system (i.e., 9.9, 15.8, and 19.8 Å). In general, the widths of the density distribution are somewhat larger than the cells of identical size for the large system. This is most pronounced for the 9.9 Å grid cell for which the half-width extends from 0.93 to 1.1 gm/cm^3 (cf. Figure 1). This finding for the small system is largely in accord with the very recent grid-based density distributions of Clark et al. [23], who used a system intermediate in size (approximately 30 000 molecules), but still some 35 times smaller in volume than the large system studied here. In the 9.9 Å-side grids, the persistence times (cf. Figure 3) are around half of those in the large system. It was found that the proportion of overall simulation time for which the low- and high-density states were present in the 472-molecule system varied in the ranges of 4%–12%, 5%–9%, and
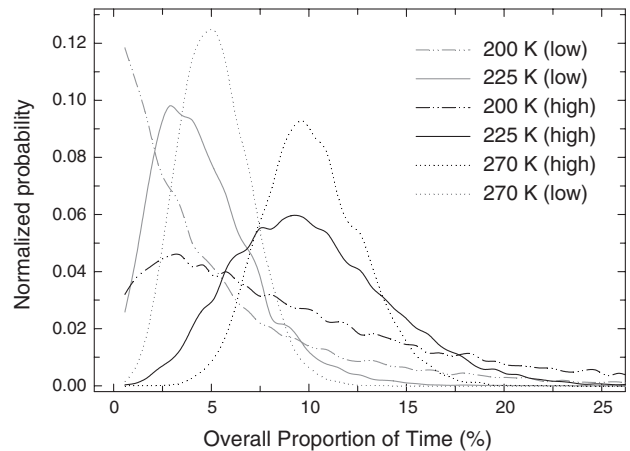

FIG. 4.   Normalized probability distributions of overall proportion of simulation time for which low- and high-densities are present in 9.9 Å-side grid elements in the 1.07×10^6-molecule system.

5%–8% for LDL and 12%–30%, 11%–20%, and 14%–18% for HDL, at 200, 225, and 270 K, respectively, which is approximately one-third larger than the corresponding quantities in the large system (cf. Figure 4). Given that the wavelength of density fluctuations is equivalent to double the side-length of the simulation box, the frequency of thermal fluctuations in the 9.9 Å-side cells would be higher in the small system, which is consistent with the observed shorter persistence times and the slightly larger proportion of overall simulation time for which such low- and high-grid-density states are present.

The self-diffusion coefficients were calculated to be 0.034, 0.18, and 1.25×10^{-9} m^2/s at 200, 225, and 270 K, respectively, from the Einstein relation [25]. The probability distributions of the potential energy per molecule, in addition to those for the average of the potential self-energies for molecules present in each 9.9 Å-side element, were also computed. They were distributed in a normal manner around approximately -11.5, -12, and -12.5 kcal/mol at 200, 225, and 270 K, and were somewhat narrower in width for the small system. The markedly slower diffusion at 200 K is consistent with a supercooled state, while the unimodal potential energy distribution throughout the molecules and grids confirms the single-phase nature of the liquid.

Through large-scale and long-time MD simulations, it is found that bulk liquid water at ambient pressure is a homogenous system. The occurrence of LDL and HDL is observed only in very short lengths scales less than 1 nm, and are transient events due to thermal density fluctuations. There is no appreciable temperature dependence down to the supercooled regime of the density distribution even for the small 9.9 Å cells. The present results reinforce the conclusion of a recent reinvestigation of the SAXS experiment that there are no inhomogeneities in ambient-pressure water structure, both above freezing and in the mildly supercooled state [23], and agree with findings for the SPC/E model in this respect of Scala *et al.* [26] and Brovchenko *et al.* [27], while providing details of the temporal existence and spatial extent of local-density regions. However, given that the objective of this study was to clarify density distributions and fluctuations in liquid water at ambient pressure, the simulations were necessarily not at the temperature and pressure conditions of the hypothesized liquid-liquid critical point; therefore, no conclusions can be drawn from this study to either challenge or support the two-liquid hypothesis [5–8]. It would appear that rationalizing the complexities of water's behavioral anomalies will remain a key scientific challenge for some time to come.

*niall.english@ucd.ie
†John.Tse@usask.ca

[1] S. Myneni *et al.*, J. Phys. Condens. Matter **14**, L213 (2002).
[2] P. Wernet *et al.*, Science **304**, 995 (2004)
[3] T. Tokushima *et al.*, Chem. Phys. Lett. **460**, 387 (2008).
[4] C. Huang *et al.*, Proc. Natl. Acad. Sci. U.S.A. **106**, 15 214 (2009).
[5] O. Mishima, Nature (London) **384**, 546 (1996).
[6] O. Mishima and H. E. Stanley, Nature (London) **396**, 329 (1998).
[7] P. G. Debenedetti and H. E. Stanley, Phys. Today **56**, No. 6, 40 (2003).
[8] P. Poole, *et al.*, Nature (London) **360**, 324 (1992).
[9] S. Harrington, R. Zhang, P. H. Poole, F. Sciortino, and H. E. Stanley, Phys. Rev. Lett. **78**, 2409 (1997).
[10] A. K. Soper, J. Teixeira, and T. Head-Gordon, Proc. Natl. Acad. Sci. U.S.A. **107**, E44 (2010).
[11] C. Huang *et al.*, Proc. Natl. Acad. Sci. U.S.A. **107**, E45 (2010).
[12] H. J. C. Berendsen, J. R. Grigera, and T. P. Straatsma, J. Phys. Chem. **91**, 6269 (1987).
[13] T. Darden *et al.*, J. Chem. Phys. **103**, 8577 (1995).
[14] W. G. Hoover, Phys. Rev. A **31**, 1695 (1985).
[15] C. J. Roberts, A. Z. Panagiotopoulos, and P. G. Debenedetti, Phys. Rev. Lett. **77**, 4386 (1996).
[16] C. Vega, J. L. F. Abascal, E. Sanz, L. G. MacDowell, and C. McBride, J. Phys. Condens. Matter **17**, S3283 (2005).
[17] I. T. Todorov and W. Smith, DL-POLY3 Molecular Simulation Code, Daresbury Laboratory, Warrington, Great Britain.
[18] S. Melchionna, G. Ciccotti, and B. L. Holian, Mol. Phys. **78**, 533 (1993).
[19] T. Bryk and A. D. J. Haymet, Mol. Simul. **30**, 131 (2004).
[20] A. Saul and W. Wagner, J. Phys. Chem. Ref. Data **18**, 1537 (1989); G. S. Kell, J. Chem. Eng. Data **20**, 97 (1975).
[21] K. A. Motakabbir and M. Berkowitz, J. Phys. Chem. **94**, 8359 (1990); H. L. Pi *et al.*, Mol. Phys., **107**, 365 (2009).
[22] L. Bosio, J. Teixeira, and M.-C. Bellissent-Funel, Phys. Rev. A **39**, 6612 (1989).
[23] G. N. I. Clark, G. L. Hora, J. Teixeira, A. K. Soper, and T. Head-Gordon, Proc. Natl. Acad. Sci. U.S.A. **107**, 14 003 (2010).
[24] F. Bruge, E. Parisi, and S. L. Fornoli, Chem. Phys. Lett., **250**, 443 (1996).
[25] M. P. Allen and D. J. Tildesley, *Computer Simulation of Liquids* (Clarendon Press, Oxford, 1989).
[26] A. Scala, F. W. Starr, E. La Nave, H. E. Stanley, and F. Sciortino, Phys. Rev. E **62**, 8016 (2000).
[27] I. Brovchenko, A. Geiger, and A. Oleinikova, J. Chem. Phys., **123**, 044515 (2005).